

Investigations of the magnetic properties and structures of the pillared perovskites, $\text{La}_5\text{Re}_3\text{MO}_{16}$ ($M = \text{Co}, \text{Ni}$)

Heather L. Cuthbert^{a,*}, John E. Greedan^{a,b}, Lachlan Cranswick^c

^aDepartment of Chemistry, McMaster University, Hamilton, Ontario, Canada L8S 4M1

^bBrockhouse Institute for Materials Research, McMaster University, Hamilton, Ontario, Canada L8S 4M1

^cThe Canadian Neutron Beam Centre, National Research Council of Canada, Chalk River Laboratories, Chalk River, Ontario, Canada

Received 24 January 2006; received in revised form 22 March 2006; accepted 26 March 2006

Available online 1 April 2006

Abstract

$\text{La}_5\text{Re}_3\text{CoO}_{16}$ and $\text{La}_5\text{Re}_3\text{NiO}_{16}$ were synthesized by solid-state reaction and studied by SQUID magnetometry, heat capacity and powder neutron diffraction measurements. These two compounds belong to a series of isostructural Re-based pillared perovskites [Chi et al. *J. Solid State Chem.* 170 (2003) 165]. Magnetic susceptibility measurements indicate apparent short-range ferri or ferromagnetic correlations and possible long-range antiferromagnetic order for $\text{La}_5\text{Re}_3\text{CoO}_{16}$ at 35 K, and at 38 and 14 K for $\text{La}_5\text{Re}_3\text{NiO}_{16}$. Heat capacity measurements of the Co compound show a lambda anomaly, typical of long-range magnetic order, at 32 K. In contrast, the Ni compound displays a broader, more symmetric feature at 12 K in the heat capacity data, indicative of short-range magnetic order. Low-temperature powder neutron diffraction revealed contrasting magnetic structures. While both show an ordering wave vector, $\mathbf{k} = (0, 0, 1/2)$, in $\text{La}_5\text{Re}_3\text{CoO}_{16}$, the Co^{2+} and Re^{5+} moments are ordered ferrimagnetically within the corner-shared octahedral layers, while the layers themselves are coupled antiferromagnetically along the *c*-axis, as also found in $\text{La}_5\text{Re}_3\text{MnO}_{16}$ and $\text{La}_5\text{Re}_3\text{FeO}_{16}$. In the case of the Ni material, the Re^{5+} and Ni^{2+} moments in the perovskite layers couple ferromagnetically and are canted 30° away from the *c*-axis, angled 45° in the *ab*-plane. The layers then couple antiferromagnetically at low temperature, a unique magnetic structure for this series. The properties of the $\text{La}_5\text{Re}_3\text{MO}_{16}$ series, with $M = \text{Mn}, \text{Fe}, \text{Co}, \text{Ni}$ and Mg are also reviewed.

© 2006 Elsevier Inc. All rights reserved.

Keywords: Pillared perovskite; Magnetic susceptibility; Neutron diffraction; Magnetic structure; Short-range and long-range magnetic order

1. Introduction

In recent years, a new family of “pillared perovskite” compounds has been discovered and investigated. This structure type has been found for oxides of molybdenum, $\text{La}_5\text{Mo}_{4-x}\text{M}_x\text{O}_{16}$ ($x = 0$ and $x \sim 0.7$ for $M = \text{Mn}, \text{Fe}, \text{Co}, \text{Mg}$) [1–3], rhenium, $\text{La}_5\text{Re}_3\text{MO}_{16}$ ($M = \text{Mn}, \text{Fe}, \text{Co}, \text{Ni}, \text{Mg}$) [4–6] and osmium, $\text{La}_5\text{Os}_3\text{MnO}_{16}$ [7]. The unit cell is pictured in Fig. 1. It consists of perovskite-like layers of corner-shared $MM'\text{O}_6$ octahedra, in which the *M* and *M'* ions are site ordered, avoiding like ion nearest neighbours. These layers are “pillared” by dimeric units of two edge-shared MO_6 octahedra. The La^{3+} ions occupy interstitial sites.

Magnetically, the pillared perovskites have displayed some interesting properties, as a result of their structure. The dimeric ‘pillars’ involve metal–metal bonding between the *4d* or *5d* transition metals and the units are diamagnetic. Within the layers, due to site ordering of the *M* and *M'* ions, both transition metals exhibit local moment behaviour with nearly spin-only values. Although the layers are separated by $\sim 10 \text{ \AA}$, long-range magnetic order exists in these compounds. For the $\text{La}_5\text{Re}_3\text{MO}_{16}$ series, the critical temperature (T_c) varies from 161 K in the Mn compound to 33 K in the Co compound [5,6]. Detailed magnetic property studies on two members of the Re series ($M = \text{Mn}$ and Fe) indicate that the magnetic structure consists of ferrimagnetically coupled layers that are coupled antiferromagnetically in three dimensions [5,6]. This current work examines the magnetic properties of two remaining Re family members, $\text{La}_5\text{Re}_3\text{CoO}_{16}$ and $\text{La}_5\text{Re}_3\text{NiO}_{16}$, in greater detail.

*Corresponding author. Fax: +1 905 521 2773.

E-mail address: cuthbehl@mcmaster.ca (H.L. Cuthbert).

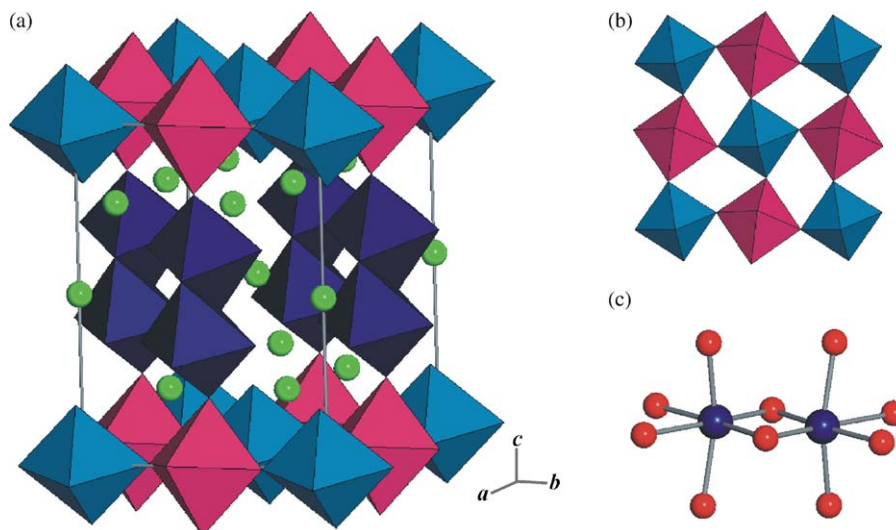


Fig. 1. Crystal structure of $\text{La}_5\text{Re}_3\text{MO}_{16}$: (a) A view of the unit cell: ReO_6 octahedra in blue, MO_6 octahedra in pink, Re_2O_{10} dimer units in dark blue and La ions in green, (b) A perovskite-like layer of corner sharing ReO_6 (blue) and MO_6 (pink) octahedra. Notice the large octahedral tilt angles away from the ideal 180° and (c) A Re_2O_{10} “pillar” of two edge-shared ReO_6 octahedra: Re atoms in dark blue and O atoms in red.

2. Experimental

2.1. Synthesis

The title compounds, $\text{La}_5\text{Re}_3\text{MO}_{16}$ ($M = \text{Co}, \text{Ni}$), were synthesized by solid-state reaction, as outlined previously [6]:



Stoichiometric amounts of the starting reagents, La_2O_3 (99.9%, Aldrich, calcined at 900°C overnight before use), ReO_3 (Rhenium Alloys), Re (Rhenium Alloys) and MO ($M = \text{CoO}$, 99.99%, Aldrich; $M = \text{NiO}$, 99.995%, CER-AC) were accurately weighed, ground together, pressed into a pellet and placed into a platinum crucible, which was sealed in a quartz tube under vacuum ($\sim 10^{-5}$ Torr). The reaction was heated to 1050°C in a tube furnace and held for 48 h. The products obtained were black powders. The non-magnetic lattice match compound for heat capacity, $\text{La}_5\text{Re}_2\text{TaMgO}_{16}$, was made in a similar manner, using stoichiometric amounts of Ta_2O_5 (99.99%, CERAC) and MgO (99.95%, Alfa Aesar) as well.

2.2. X-ray and neutron diffraction

X-ray diffraction data were collected using a Guinier-Hagg camera with $\text{CuK}\alpha_1$ radiation ($\lambda = 1.5406 \text{ \AA}$) and high-purity silicon powder as an internal reference. In addition, X-ray diffraction data suitable for Rietveld refinement was obtained from a Bruker D8 diffractometer using $\text{CuK}\alpha_1$ radiation from 10° to 80° in the 2θ range. A step size of 0.025° and a step time of 12 s were employed.

Variable temperature powder neutron diffraction measurements were performed on the C2 diffractometer operated by the Canadian Neutron Beam Centre at NRC

Chalk River Laboratories. The crystal structure data (285 K) were collected at a wavelength of 1.32917 \AA in the angular range of $12^\circ \leq 2\theta \leq 113^\circ$ with 0.1° steps. Similarly, the magnetic structure data (variable temperatures from 4 K) were measured at a longer wavelength of 2.36957 \AA in the range $5^\circ \leq 2\theta \leq 85^\circ$ with 0.1° intervals.

2.3. Magnetic data

Magnetic measurements were collected using a Quantum Design MPMS SQUID magnetometer. Zero-field-cooled and field-cooled (ZFC/FC) magnetic susceptibility data from 2 to 300 K and isothermal magnetization measurements from 0 to 5 T were recorded on samples encased in gelatin capsules.

2.4. Heat capacity

Heat capacity data were measured using the heat capacity probe in an Oxford MagLab at McMaster University. Thin sample blocks of approximately 10 mg were prepared by repressing and resintering a portion of the previously synthesized product. Sample structure integrity was verified by powder X-ray diffraction (Guinier). The sample block was mounted onto a sapphire measurement chip with Apeizon grease. Contributions to the measured heat capacity by the grease and sample chip were accounted for.

3. Results and discussion

3.1. Structural characterization

The structures of both title compounds were verified by their Guinier powder patterns, which matched well with the

patterns obtained for the same compositions synthesized previously [6]. Further structure characterization was accomplished through Rietveld refinement of room temperature powder X-ray ($\text{La}_5\text{Re}_3\text{NiO}_{16}$) and neutron ($\text{La}_5\text{Re}_3\text{CoO}_{16}$) diffraction data using WINPLOTR in the FULLPROF program [8]. The unit cell constants and agreement indices are displayed in Table 1, with the previously published values in square parentheses. From these results, it is clear that the synthesized compounds are $\text{La}_5\text{Re}_3\text{CoO}_{16}$ and $\text{La}_5\text{Re}_3\text{NiO}_{16}$. This structure type is illustrated in Fig. 1 and has been discussed previously. The short Re–Re distance found in the dimer (2.380(8) Å for Co and 2.419(6) Å for Ni) is indicative of a Re–Re double bond, which would pair the Re^{5+} electrons and quench the magnetic moment within the pillars. The only magnetic ions in these compounds are Re^{5+} ($S = 1$) and M^{2+} (Co, $S = 3/2$; Ni, $S = 1$) within the perovskite layers.

3.2. Magnetic measurements

3.2.1. $\text{La}_5\text{Re}_3\text{CoO}_{16}$

ZFC/FC magnetic susceptibility measurements from 5–300 K at a field of 0.05 T and from 2 to 200 K at fields of 2.0 and 5.0 T, respectively are shown in Fig. 2. Data acquired at the lowest applied field (0.05 T) show a large cusp at 35 K and two smaller, broader shoulders centred at 75 and 100 K, respectively. The sharp feature is attributed to long-range antiferromagnetic order (with an ordering temperature, T_c of 35 K), while the features at higher temperatures are indicative of short-range magnetic correlations. The ZFC and FC data begin to diverge at approximately 140 K. This result is comparable to the ZFC–FC susceptibility (χ) data measured previously [6]. However, the small feature at 100 K did not appear in the earlier measurements. A plot of χT versus temperature, shown in Fig. 3, shows this feature more prominently. The horizontal line in the plot represents the calculated spin-only Curie constant for the combination of Re^{5+} ($S = 1$;

$C_{\text{SO}} = 1.00 \text{ emu/mol K}$) and Co^{2+} ($S = 3/2$; $C_{\text{SO}} = 1.87 \text{ emu/mol K}$) ions. At higher temperatures ($\sim 300 \text{ K}$), χT approaches this value, which is as expected if the compound obeys the Curie–Weiss law in that temperature regime. The new, broad peak at 100 K may represent very short-range intraplanar magnetic order, perhaps in the form of one-dimensional chains. The sharper cusp at 35 K is even more pronounced, which is indicative of short-range ferro- or ferrimagnetic correlations.

When the field is increased to 2.0 T, the ZFC–FC divergence moves to a lower temperature (20 K), the sharp cusp at 35 K broadens significantly in the ZFC data, and the weaker features are lost. Finally, at 5.0 T, the ZFC–FC divergence is negligible and all the features are gone. The 5.0 T curve suggests ferrimagnetic behaviour, with a saturation moment of about $1.3(1)\mu_{\text{B}}$. This is slightly larger than the expected spin-only saturation moment ($1.0\mu_{\text{B}}$) for ferrimagnetically coupled Co^{2+} ($S = 3/2$) and Re^{5+} ($S = 1$) moments. The magnetic moment of Co^{2+} ions often exceed the spin-only value and the Re^{5+} moment is expected to be smaller, due to orbital contributions. However, this experimental moment is well below that calculated for ferromagnetically coupled Co^{2+} ($S = 3/2$) and Re^{5+} ($S = 1$) moments within the layers ($5.0\mu_{\text{B}}$).

From the crystal structure of $\text{La}_5\text{Re}_3\text{CoO}_{16}$, there are two different types of magnetic interaction—intraplanar and interplanar. Intraplanar magnetic coupling would involve Re–O–Co superexchange pathways within the perovskite layer, and would be relatively strong because of geometry (comparatively short distances and angles of approximately 155°). However, interplanar coupling would require magnetic superexchange through the diamagnetic Re_2O_{10} dimer and over much greater a distance (approximately 10 Å). This type of interaction would be expected to be much weaker, and could be overcome with the modest magnetic field applied here, such as 5.0 T.

Isothermal magnetization data at temperatures of 2, 32, 40, 55, 80 and 200 K were collected on $\text{La}_5\text{Re}_3\text{CoO}_{16}$ for

Table 1
Unit cell parameters and agreement factors for the structural refinement of diffraction data for $\text{La}_5\text{Re}_3\text{CoO}_{16}$ and $\text{La}_5\text{Re}_3\text{NiO}_{16}$

Compound	$\text{La}_5\text{Re}_3\text{CoO}_{16}$	$\text{La}_5\text{Re}_3\text{NiO}_{16}$
Data source	Neutron	X-ray
Space group	C-1	C-1
Cell parameters	$a = 7.9621(8) \text{ \AA}$ [7.9694(7) Å] $b = 7.9957(8) \text{ \AA}$ [8.0071(8) Å] $c = 10.172(1) \text{ \AA}$ [10.182(1) Å] $\alpha = 90.248(5)^\circ$ [90.248(4)°] $\beta = 94.975(4)^\circ$ [94.980(4)°] $\gamma = 89.977(8)^\circ$ [89.983(6)°]	$a = 7.9280(4) \text{ \AA}$ [7.9383(4) Å] $b = 7.9888(4) \text{ \AA}$ [7.9983(5) Å] $c = 10.1585(5) \text{ \AA}$ [10.1732(6) Å] $\alpha = 90.274(2)^\circ$ [90.287(3)°] $\beta = 94.876(2)^\circ$ [94.864(3)°] $\gamma = 89.967(3)^\circ$ [89.968(4)°]
Agreement factors	$R_p = 0.0282$ $wR_p = 0.0380$ $\chi^2 = 2.02$ $R_B = 0.0543$	$R_p = 0.128$ $wR_p = 0.168$ $\chi^2 = 1.22$ $R_B = 0.0708$

The literature values are shown in square parentheses.

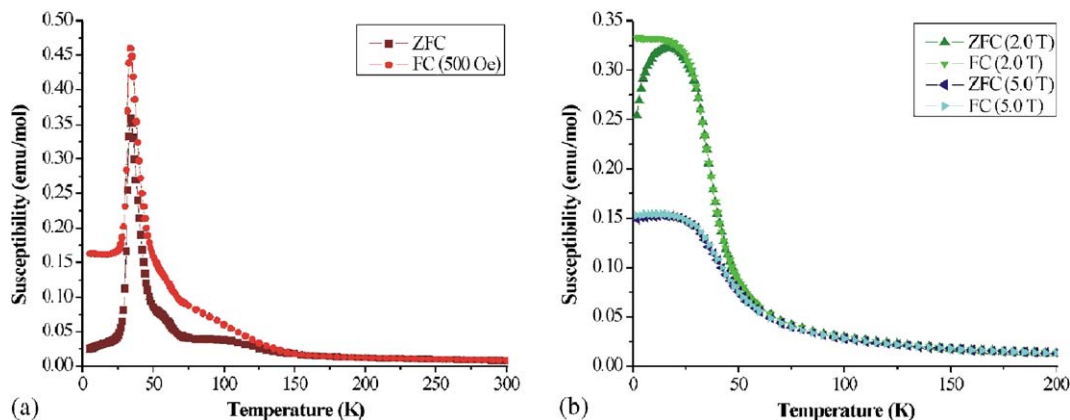


Fig. 2. ZFC (darker shade) and FC (lighter shade) magnetic susceptibility measurements of $\text{La}_5\text{Re}_3\text{CoO}_{16}$ with applied fields of (a) 0.05 T (red) and (b) 2.0 T (green) and 5.0 T (blue).

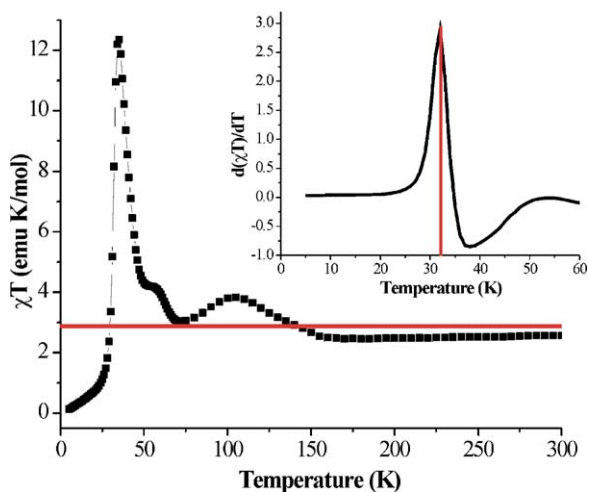


Fig. 3. χT versus T plot of $\text{La}_5\text{Re}_3\text{CoO}_{16}$ using the ZFC data only. The horizontal line is the sum of the calculated spin only Curie constants for Re^{5+} ($S = 1$; $C_{\text{SO}} = 1.00 \text{ emu/mol K}$) and Co^{2+} ($S = 3/2$; $C_{\text{SO}} = 1.87 \text{ emu/mol K}$). Inset—Fisher heat capacity of $\text{La}_5\text{Re}_3\text{CoO}_{16}$ calculated using the ZFC magnetic susceptibility data. The vertical line denotes the peak centre. Note the peak asymmetry.

fields between 0 and 5.0 T and are shown in Fig. 4. At 2 K, the magnetization increases sharply at an applied field of 6500 Oe, and curves gradually to approach a saturation moment of $1.3 \mu_{\text{B}}$ at 5.0 T. Again, this value matches the saturation moment obtained from the 5.0 T ZFC/FC susceptibility data and is indicative of ferrimagnetically coupled moments through out the structure. There is very strong hysteresis present at 2 K, and a rather large remnant magnetization of $0.6 \mu_{\text{B}}$. The sharp increase at low field is interpreted as the onset of a transition analogous to metamagnetism, in which the weak antiferromagnetic interlayer coupling is reversed by the applied field. A slight hysteresis persists in this compound up to 40 K. The 32 K data show a more gradual upturn at 3000 Oe, and then begin to level off. The 40 K data also curve gradually upwards, however at 55, 80 and 200 K, the signal is linear.

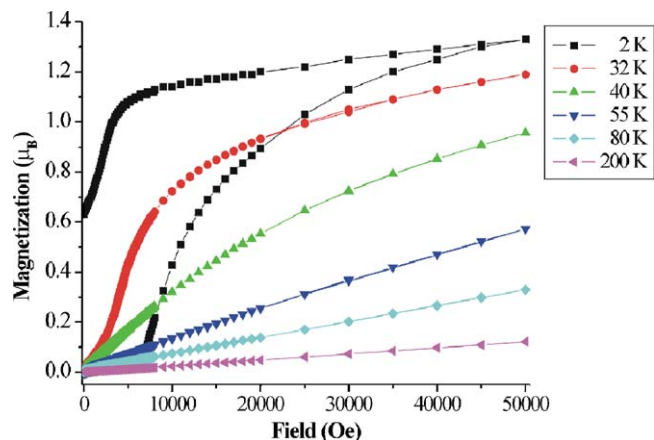


Fig. 4. Isothermal magnetization versus applied field data for $\text{La}_5\text{Re}_3\text{CoO}_{16}$. Note the large residual magnetization at 2 K and the sharp jumps at low applied field in the 2 and 32 K curves.

At these higher temperatures, the data are consistent with paramagnetism. All of these responses corroborate the hypothesis that T_{c} for this compound is 35 K.

Heat capacity data collected from 10 to 50 K on $\text{La}_5\text{Re}_3\text{CoO}_{16}$ in the absence of a magnetic field and with a 7 T field applied, as well as the heat capacity measured for the non-magnetic lattice match compound, $\text{La}_5\text{Re}_2\text{TaMgO}_{16}$ are pictured in Fig. 5. From Fig. 6, subtraction of the lattice component discloses a lambda-like anomaly, albeit somewhat broad, with a peak at 32 K. This signals the onset of relatively long-range magnetic order. The inset graph in Fig. 3 shows the so-called Fisher heat capacity for $\text{La}_5\text{Re}_3\text{CoO}_{16}$. There is one clear peak, whose maximum is at about 32 K and whose shape is quite asymmetric and lambda-like. Both of these features indicate good agreement between the heat capacity and SQUID magnetometry measurements. Application of a 7 T field significantly decreases the height of the heat capacity anomaly of $\text{La}_5\text{Re}_3\text{CoO}_{16}$ and broadens it, indicating that the transition to long-range magnetic order is field dependent. As

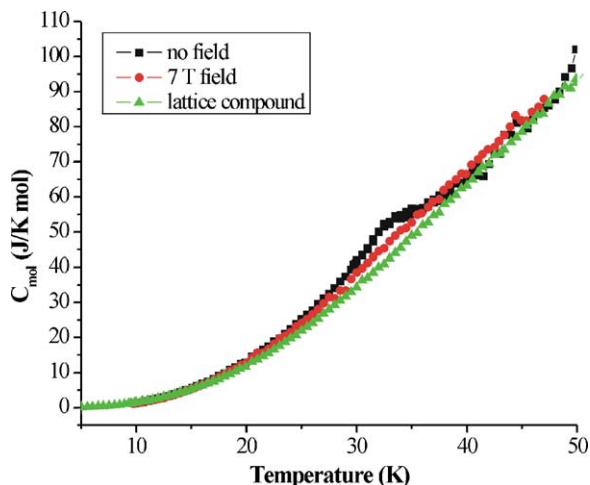


Fig. 5. Heat capacity measurements of $\text{La}_5\text{Re}_3\text{CoO}_{16}$ with no field applied (black squares) and in a 7.0 T field (red circles). The heat capacity measured for the non-magnetic lattice match compound is denoted by green triangles.

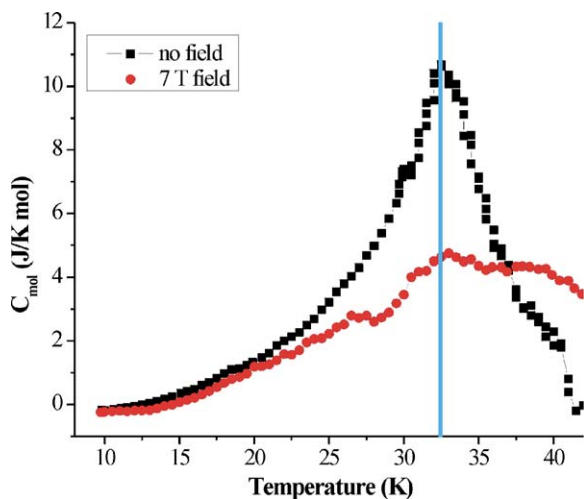


Fig. 6. Magnetic component of the heat capacity of $\text{La}_5\text{Re}_3\text{CoO}_{16}$, in zero-applied field (black squares) and in a 7 T field (red circles). The blue line denotes the peak centre. Note the lambda-like shape.

noted previously from the SQUID magnetometry data, the interplanar magnetic coupling is relatively weak, and can be overcome by modest magnetic fields.

Integration of the area under the curve for the zero applied field measurements results in an estimation of the change in entropy associated with this magnetic transition,

$$\Delta S = \int_0^T (C_{\text{mol}}/T) dT \quad (2)$$

yielding $\Delta S = 3.56 \text{ J/mol}$. This value is only 17% of the 20.66 J/mol expected for Re^{5+} ($S = 1$) and Co^{2+} ($S = 3/2$) moments and indicates that most of the magnetic entropy is lost in the intraplanar short-range order.

Variable temperature powder neutron diffraction measurements were also performed on $\text{La}_5\text{Re}_3\text{CoO}_{16}$ to

elucidate its magnetic structure. Fig. 7 shows low angle neutron diffraction data of this compound at selected temperatures, to highlight the development of the new magnetic Bragg reflections. At 5 K, the two high intensity peaks (at $2\theta = 24.7^\circ$ and 25.5°) can be indexed to a magnetic unit cell with ordering vector, $\mathbf{k} = (0, 0, 1/2)$ (i.e. $a_{\text{mag}} = a$, $b_{\text{mag}} = b$, $c_{\text{mag}} = 2c$, where a , b , c are the axes of the structural unit cell). This magnetic unit cell is the same as $\text{La}_5\text{Re}_3\text{MnO}_{16}$ [5] and $\text{La}_5\text{Re}_3\text{FeO}_{16}$ [6]. For these materials, the magnetic structure consists of ferrimagnetically coupled perovskite layers, coupled antiferromagnetically along the c -axis, which is depicted in Fig. 8.

Using the same model, attempts were made to refine the magnetic structure of $\text{La}_5\text{Re}_3\text{CoO}_{16}$. However, due to a high degree of correlation between the Re^{5+} ($S = 1$) and Co^{2+} ($S = 3/2$) moments, their values could not be refined independently. The best fit, as seen in the difference plot and R_{mag} values, was obtained when the moments were fixed parallel to the c -axis at 1.5 and $2.5 \mu_B$ for the Re and Co, respectively, as shown in Fig. 9. The magnitudes of these moments are not unreasonable, and are close to the spin-only values for these ions. A plot of the relative intensity of the $(1, 1, 1/2)/(1, -1, 1/2)$ magnetic peak as a function of temperature is displayed in Fig. 10. The critical temperature of 35 K suggested by neutron diffraction is consistent with both the SQUID magnetometry and heat capacity results. Note also that the magnetic reflections appear to be resolution limited (they are not obviously broader than the chemical structure reflections) indicating that the correlation length for magnetic order is at least 100 \AA or more.

3.2.2. $\text{La}_5\text{Re}_3\text{NiO}_{16}$

ZFC and FC magnetic susceptibility measurements at fields of 0.05, 2.0 and 5.0 T are plotted in Fig. 11. The data collected at the lowest field ranges from 5 to 300 K, whereas

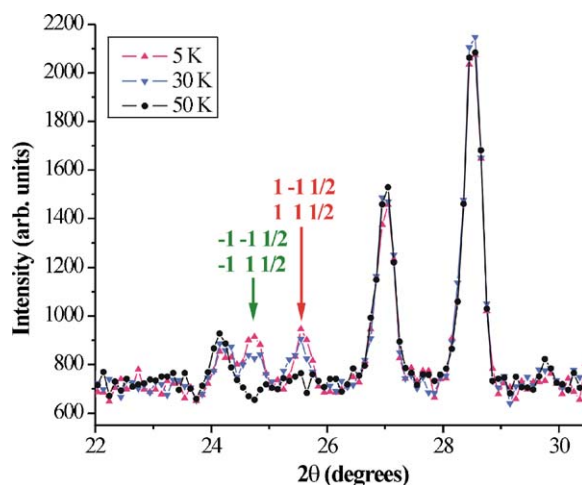


Fig. 7. Powder neutron diffraction patterns of $\text{La}_5\text{Re}_3\text{CoO}_{16}$ at 5 K (pink triangles), 30 K (blue inverted triangles) and 50 K (black circles). The peaks marked with arrows are the two new magnetic Bragg reflections, indexed as indicated.

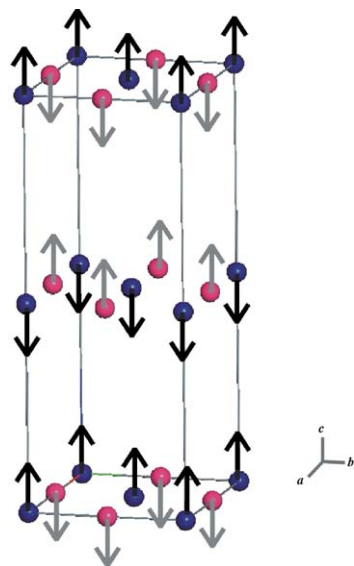


Fig. 8. Magnetic structure of $\text{La}_5\text{Re}_3\text{CoO}_{16}$, showing the moments on the Re atoms (blue spheres, black arrows) and Co atoms (pink spheres, grey arrows).

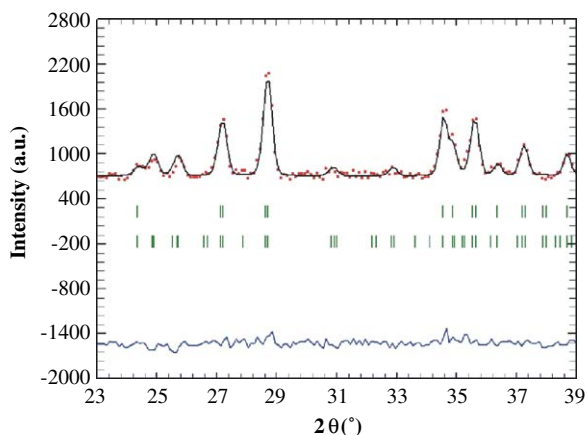


Fig. 9. Rietveld refinement of the low angle powder neutron diffraction data for $\text{La}_5\text{Re}_3\text{CoO}_{16}$ at 5 K. The red circles are the experimental data; the black line is the calculated pattern; the top green tick marks denote the structural Bragg reflections; the bottom green tick marks are the magnetic Bragg reflections and the blue line is the difference plot. Only the crystal structure was refined, the magnetic structure was simulated as described in the text.

the 2.0 and 5.0 T data sets were collected from 2 to 200 K. At 0.05 T, the ZFC and FC curves begin to diverge at approximately 40 K. There are two prominent cusps below this temperature, centred at 38 and 14 K, respectively, which are indicative of magnetic ordering. As the peak at 38 K is suppressed in the FC data, the cusp at 14 K is attributed to the onset of relatively long-range antiferromagnetic order. This is in contrast to the previously reported T_c of 36 K for $\text{La}_5\text{Re}_3\text{NiO}_{16}$ [6]. A plot of χT versus T is shown in Fig. 12 with the Fisher heat capacity included in the inset. Similar to the case with the Co phase, a sharp upturn is seen below 50 K with a maximum at 36 K

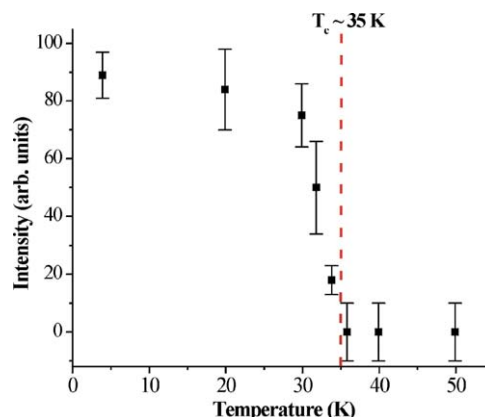


Fig. 10. Temperature dependence of the magnetic peak indexed as $(1,1,1/2)/(1,-1,1/2)$ in $\text{La}_5\text{Re}_3\text{CoO}_{16}$ indicating the critical temperature of ~ 35 K.

and a clear inflection point at 14 K. However, the broad maxima above 50 K seen in the Co data are absent. These observations are consistent with short-range ferri- or ferromagnetic order. Here again the horizontal line on the graph is the sum of the calculated spin-only Curie constants for Re^{5+} ($S = 1$; $C_{\text{SO}} = 1.00$ emu/mol K) and Ni^{2+} ($S = 1$; $C_{\text{SO}} = 1.00$ emu/mol K). For $\text{La}_5\text{Re}_3\text{NiO}_{16}$, even at 300 K, the value of χT does not reach this line.

When the field is increased to 2.0 T, the divergence between the two curves moves to lower temperature (7 K), and the peak associated with long-range order broadens and moves to lower temperature (6 K) as well. By 5.0 T, there is no longer a divergence between the ZFC and FC curves and the signal suggests ferro- or ferrimagnetic ordering of the moments in the perovskite layers. Again, as with the Co analogue, it appears that the interplanar coupling is relatively weak and can be overcome with laboratory magnetic fields. However, the supposed “saturation moment” obtained from the 5.0 T data is about $0.9(1) \mu_B$, which is much lower than the value calculated for ferromagnetically coupled Re^{5+} ($S = 1$) and Ni^{2+} ($S = 1$) layers ($4.0 \mu_B$), but of course, much larger than the $\sim 0 \mu_B$ expected for ferrimagnetic coupling. This suggests that $\text{La}_5\text{Re}_3\text{NiO}_{16}$ has not reached saturation at this field. This compound may have unique magnetic properties, such as a much higher anisotropy field than seen in the other isostructural-pillared perovskites.

Magnetization curves were collected from 0 to 5.0 T at temperatures of 2, 12, 30, 42 and 100 K and are pictured in Fig. 13. The 2 K data show a large hysteresis (which persists up to 30 K) but virtually no remnant magnetization. Unlike the Co compound, there are no sharp increases in the magnetization, but rather a smooth S-shaped curve, with an inflection point at about 1.5 T. This may be indicative of a metamagnetic transition as in the Co phase, albeit with a much higher critical field. Also, the curve does not reach saturation at 5.0 T. The 12 K magnetization curve maintains the S-shape, however by

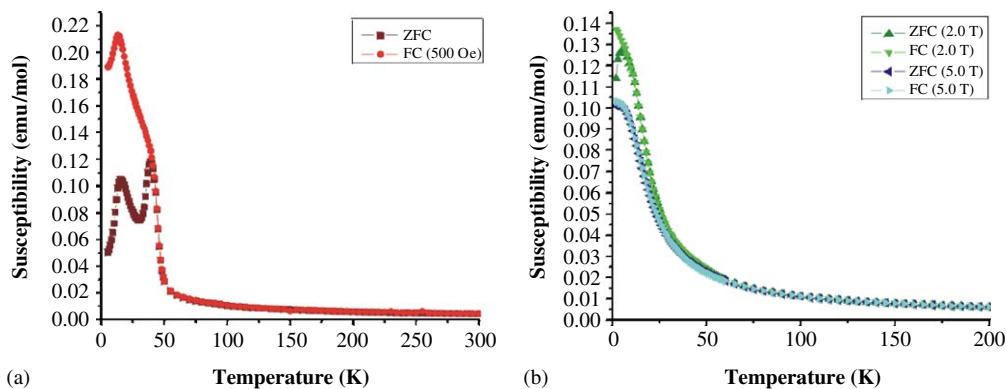


Fig. 11. ZFC (darker shade) and FC (lighter shade) magnetic susceptibility measurements of $\text{La}_5\text{Re}_3\text{NiO}_{16}$ with applied fields of (a) 0.05 T (red) and (b) 2.0 T (green) and 5.0 T (blue).

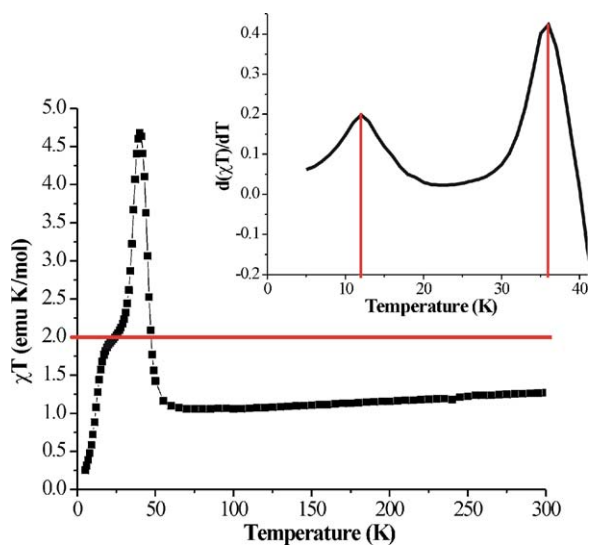


Fig. 12. χT versus T plot of $\text{La}_5\text{Re}_3\text{NiO}_{16}$ using the ZFC data only. The horizontal line is the sum of the calculated spin only Curie constants for Re^{5+} ($S = 1$; $C_{\text{SO}} = 1.00 \text{ emu/mol K}$) and Ni^{2+} ($S = 1$; $C_{\text{SO}} = 1.00 \text{ emu/mol K}$). Inset—Fisher heat capacity of $\text{La}_5\text{Re}_3\text{NiO}_{16}$ calculated using the ZFC magnetic susceptibility data. The vertical line denotes the peak centres.

30 K, the data are linear, indicating paramagnetism, and corroborating the assignment of T_c as 14 K.

Heat capacity measurements on $\text{La}_5\text{Re}_3\text{NiO}_{16}$ were also collected from about 5–50 K, with no field applied and in a 7.0 T field. The two data sets, along with the heat capacity of the lattice match compound, $\text{La}_5\text{Re}_2\text{TaMgO}_{16}$ are shown in Fig. 14. After subtraction of the lattice component, the heat capacity of $\text{La}_5\text{Re}_3\text{NiO}_{16}$ pictured in Fig. 15 shows one small anomaly present with a maximum near 12 K. The shape of the 12 K feature is not lambda-like, but relatively symmetric, suggesting that the magnetic ordering present in this compound has a finite correlation length. Due to instrument restrictions, it was not possible to collect heat capacity data below 5 K, which may have clarified the peak shape. The unusual peak shape notwithstanding, smooth transient data collected on this com-

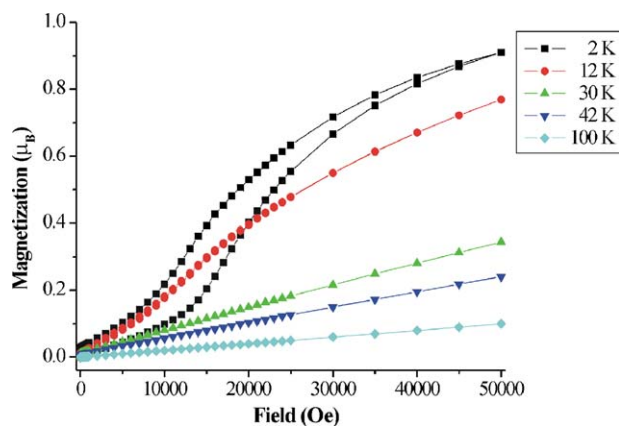


Fig. 13. Isothermal magnetization versus applied field data for $\text{La}_5\text{Re}_3\text{NiO}_{16}$.

pound demonstrates that it has good overall thermal contact, despite not being a single crystal or a dense pellet. Heat capacity data were also collected on a mixture of $\text{La}_5\text{Re}_3\text{NiO}_{16}$ and metallic silver powder (25% by weight) in an effort to improve the thermal contact. The shape and position of the anomaly remained unchanged. However, the temperature of the peak centre agrees well with the estimate of T_c for this compound from the magnetic susceptibility and magnetization data. The Fisher heat capacity of $\text{La}_5\text{Re}_3\text{NiO}_{16}$ is displayed in Fig. 12 (inset) showing two peaks at about 12 and 36 K. Interestingly, the peak at 12 K is again relatively symmetric in shape, although data were not collected below 5 K. There are no other features in the thermally derived heat capacity of $\text{La}_5\text{Re}_3\text{NiO}_{16}$ at higher temperatures (for example, at 38 K), indicating the assignment of T_c as 14 K is correct. This contrasts with the assignment of T_c as 36 K for this compound reported previously [6].

Application of a 7.0 T field appears to decrease the height of the anomaly, broaden it significantly and shift the peak maximum. The strong field dependence of this feature suggests that the transition to long-range magnetic order

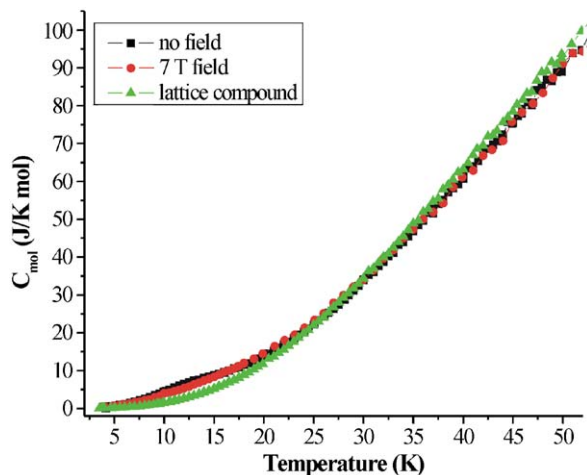


Fig. 14. Heat capacity measurements of $\text{La}_5\text{Re}_3\text{NiO}_{16}$ in zero-applied field (black squares) and in a 7.0 T field (red circles). The heat capacity measured for the non-magnetic lattice match compound is denoted by green triangles.

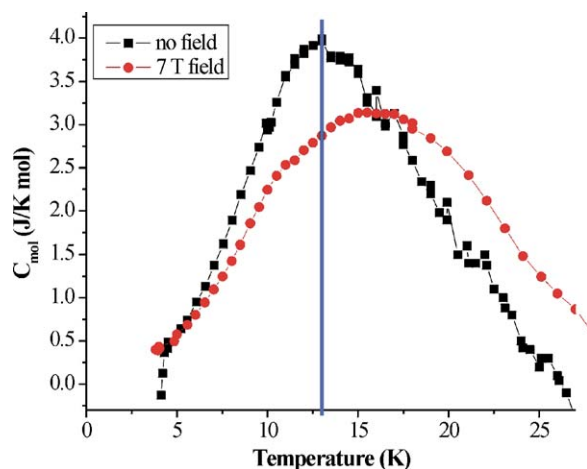


Fig. 15. Magnetic component of the heat capacity of $\text{La}_5\text{Re}_3\text{NiO}_{16}$, in zero field (black squares) and in a 7 T field (red circles). The blue line denotes the peak centre.

involves a relatively weak coupling (i.e. interlayer). Integration of C_{mol}/T with respect to temperature leads to a change of entropy of 3.68 J/mol for $\text{La}_5\text{Re}_3\text{NiO}_{16}$. This is comparable to the value obtained for $\text{La}_5\text{Re}_3\text{CoO}_{16}$. The calculated entropy for this compound, with Re^{5+} moments ($S = 1$) and Ni^{2+} moments ($S = 1$) is 18.27 J/mol, which is considerably higher than the experimental value. Again, as with the Co compound, most of the entropy is removed due to short-range intraplanar correlations prior to the onset of relatively long-range three-dimensional magnetic order.

Low-temperature powder neutron diffraction measurements were taken to determine the magnetic structure of $\text{La}_5\text{Re}_3\text{NiO}_{16}$, and the diffraction data at 4 and 50 K are plotted in Fig. 16. Unlike the Co compound, there is only one very weak, new magnetic Bragg peak at very low angle ($6.5^\circ 2\theta$). This reflection can also be indexed to a

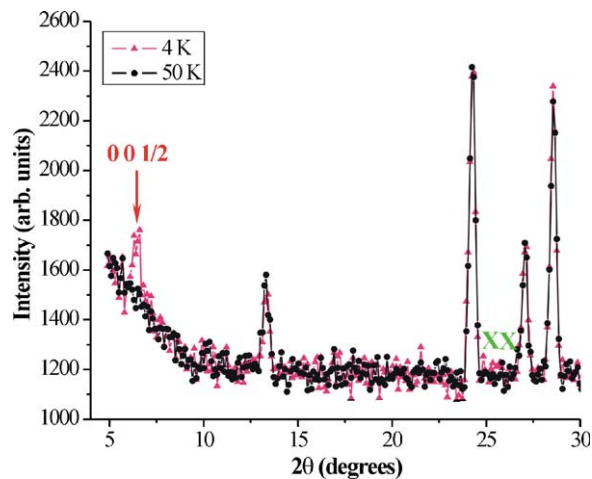


Fig. 16. Powder neutron diffraction patterns of $\text{La}_5\text{Re}_3\text{NiO}_{16}$ at 4 K (pink triangles) and 50 K (black circles). The peak marked with an arrow is the new magnetic Bragg reflection, indexed accordingly. Note the absence of reflections of the type $(\pm 1, \pm 1, 1/2)$ and $(\pm 1, \pm 1, 3/2)$, (green 'X's).

magnetic unit cell with ordering vector, $\mathbf{k} = (0, 0, 1/2)$. However, the peak index is $(0, 0, 1/2)$, which indicates that the moments within the layer are not oriented parallel to the c -axis, unlike most of the other members of the pillared perovskite family studied to date. An exception is $\text{La}_5\text{Re}_3\text{MnO}_{16}$, where the Mn moments are canted $\sim 18^\circ$ with respect to the c -axis [5]. In addition, no magnetic reflections of indices $(h, k, l/2)$ and $(h, k, 3l/2)$, ubiquitous at higher angles in the magnetic neutron diffraction patterns of the other phases, are present in the Ni data. These reflections are diagnostic of intraplanar ferrimagnetic correlations.

Attempts to refine the magnetic neutron diffraction data were hampered due to background problems, the paucity of data and the same high level of correlation between the Re and Ni moments as encountered for the Co compound. However, a plausible magnetic structure model, guided by simulations, was found and is pictured in Fig. 17. In all models tested, the intralayer coupling was ferromagnetic and the interlayer coupling was antiferromagnetic along the c direction and with the moments inclined away from the c -axis, as dictated by the details of the diffraction pattern. Due to the aforementioned correlation problem, the moments of the two magnetic ions, Re^{5+} ($S = 1$) and Ni^{2+} ($S = 1$), were fixed at 1.5 and 1.8 μ_B , respectively, which are close to the spin-only moments for each ion. Then, the projection angles of the net moment with respect to the crystallographic axes were varied. The best fit, determined by monitoring R_{mag} , was obtained when the net moment was canted $30(3)^\circ$ away from the c -axis with a projection of $45(5)^\circ$ in the ab plane. Not surprisingly, results were less sensitive to the ab plane angle. Of course, given the constraints, this is not a unique solution. Information from single crystal magnetization studies would be needed to fix the canting angles and the net moment values.

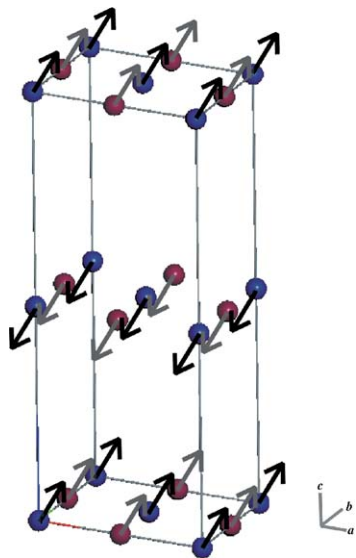


Fig. 17. Possible magnetic structure of $\text{La}_5\text{Re}_3\text{NiO}_{16}$, showing the moments on the Re atoms (blue spheres, black arrows) and Ni atoms (purple spheres, grey arrows).

4. Summary and conclusions

Detailed magnetic property studies on two isostructural-pillared perovskites, $\text{La}_5\text{Re}_3\text{CoO}_{16}$ and $\text{La}_5\text{Re}_3\text{NiO}_{16}$, has revealed some unique and unexpected results. As with the other members of this family, both compounds show evidence of three-dimensional magnetic order from SQUID magnetometry, powder neutron diffraction and heat capacity measurements, despite an interplanar separation of over 10 Å. From these studies it is now possible to assign a T_c of 14 K for the $\text{La}_5\text{Re}_3\text{NiO}_{16}$ compound and $T_c \sim 35$ K for the Co phase. In addition, the appearance of the heat capacity peaks differs between the two compounds. $\text{La}_5\text{Re}_3\text{CoO}_{16}$ shows a more typical, asymmetric lambda shape (albeit somewhat broadened), while the peak shape for the Ni material is very broad and more symmetric. This suggests that the length scale for interplanar three dimensional order in the Ni phase is shorter than for the Co compound.

Both the magnetic susceptibility and the heat capacity are strongly affected by the application of relatively modest magnetic fields. Isothermal magnetization data indicate the presence of metamagnetic-like transitions at ~ 0.65 T for $\text{La}_5\text{Re}_3\text{CoO}_{16}$ and ~ 1.5 T for $\text{La}_5\text{Re}_3\text{NiO}_{16}$. As well, the magnetic anisotropy appears to be much stronger in the Ni phase as evidenced by a lack of saturation even in fields up to 5.0 T. The onset of metamagnetism at such low applied fields is taken as evidence for relatively weak interplanar exchange coupling.

Powder neutron diffraction measurements showed that the Co series member has a magnetic structure similar to $\text{La}_5\text{Re}_3\text{MnO}_{16}$ and $\text{La}_5\text{Re}_3\text{FeO}_{16}$ [5,6]. The Re^{5+} and M^{2+} moments within the layers are coupled ferrimagnetically, and the layers are coupled antiferromagnetically.

In contrast, the magnetic structure of $\text{La}_5\text{Re}_3\text{NiO}_{16}$ is unique among the pillared perovskites. Within the layers, the two moments are ordered ferromagnetically, angled 45° in the ab plane and canted 30° away from the c -axis. The layers are then coupled antiferromagnetically.

At this stage it is useful to review the known magnetic properties of the $\text{La}_5\text{Re}_3\text{MO}_{16}$ series. In Table 2, a slightly revised version of a table of collected magnetic data (Table 7 from Chi et al. [6]) is presented.

In particular, the value for T_c of the $M = \text{Ni}$ compound is modified in light of these new results and new Curie–Weiss fits were made for the $M = \text{Ni}$ and Mg phases. The revision of the T_c value for the Ni phase results in the existence of two categories of materials in terms of the T_c/S^2 value (column 3, Table 2). Both Mn and Fe show relatively large values, around 30, while this ratio is halved for Co and Ni. The T_c/S^2 ratio is, within the mean field approximation, proportional to the product of J_{inter} (the intraplanar exchange coupling) and $(\zeta_{\text{intra}})^2$, the square of the intraplanar correlation length [9]. However, the two contributions cannot be separated without an independent measurement.

In addition, after re-examining the data for the $M = \text{Mg}$ and Ni phases, it was noted that the χ^{-1} vs. T plots were not linear throughout the temperature range 300–600 K. In such cases, an ambiguity arises concerning the fitting procedure. For example, in the previous study [6], only high-temperature data which appeared to be linear over a limited range were fit to the Curie–Weiss law. Alternatively, a fit can be made using a wider temperature range by including a TIP term (arising, presumably, from van Vleck-type contributions) to account for the curvature. The results from the latter approach are listed in Table 2 along with the previous values in square brackets.

As expected, the values for the Curie constant (C) and the Weiss temperature (θ) are somewhat reduced from those reported previously, but are not unreasonable. The $M = \text{Mg}$ compound is key here as only Re–Re exchange is involved. Note that θ , which is the weighted, algebraic sum of all of the magnetic exchange pathways, is very large and negative (~ -400 to -600 K) for this phase, regardless of the fitting method used. For $M^{2+} = \text{Mn}, \text{Fe}, \text{Co}$ and Ni , the θ values are much less negative. This implies that at least some of the Re– M magnetic interactions are ferromagnetic, which is consistent with the Goodenough–Kanamori rules for magnetic superexchange [10,11]. Re^{5+} has only t_{2g} electrons while all of the M^{2+} cations have half-occupied e_g levels. Magnetic exchange from half-filled e_g (on M^{2+}) to empty e_g (on Re^{5+}) should always be ferromagnetic. Thus, one might normally expect to find the magnetic structure seen for the $\text{La}_5\text{Re}_3\text{NiO}_{16}$ material with ferromagnetic intralayer correlations. However, somehow, the magnetic ground state that results in the majority of cases shows overall ferrimagnetic order within the planes. It is fair to say that the origin of the magnetic structures observed for these

Table 2

Magnetic data for the $\text{La}_5\text{Re}_3\text{MO}_{16}$ series. The values in square parentheses are from Chi et al.[6].

<i>M</i>	θ (K)	T_c (K)	T_c/S^2 (K)	C_{expt} (emu K/mol)	C_{so}^{a} (emu K/mol)
Mn	[−48(5)]	[161]	[26]	[4.43(4)]	5.38
Fe	[−84(4)]	[155]	[39]	[3.60(2)]	4.00
Co	[−71.2(5)]	35 [33]	16 [15]	[3.578(3)]	2.87
Ni	−74(4) [−217(3)]	14 [36,14]	14 [36]	1.49(2) [2.29(1)]	2.00
Mg	−424(28) [−575(12)]	—	—	0.81(5) [1.00(1)]	1.00

^aThe Curie constant based on the spin-only model.

Re-based pillared perovskites is not well understood and a deeper analysis is called for.

Note added in proof

To view colour versions of the figures that respond to the colour mentioned in their legends, please see the online version of this article at www.sciencedirect.com.

Acknowledgments

The authors wish to thank the Natural Sciences and Engineering Research Council (NSERC) of Canada for a Doctoral Postgraduate Scholarship (HLC) and for a research grant (JEG). We also thank Dr. Paul Dube and Dr. Graeme Luke for their assistance and use of instruments in the magnetic and heat capacity measurements.

References

- [1] M. Ledesert, P. Labbe, W.H. McCarroll, H. Leligny, B. Raveau, *J. Solid State Chem.* 105 (1993) 143.
- [2] K.V. Ramanujachary, M. Greenblatt, W.H. McCarroll, J.B. Goodenough, *Mater. Res. Bull.* 28 (1993) 1257.
- [3] K.V. Ramanujachary, S.E. Lofland, W.H. McCarroll, T.J. Emge, M. Greenblatt, *J. Solid State Chem.* 164 (2002) 60.
- [4] C.R. Wiebe, A. Gourrier, T. Langet, J.F. Britten, J.E. Greedan, *J. Solid State Chem.* 151 (2000) 31.
- [5] A.E.C. Green, C.R. Wiebe, J.E. Greedan, *Solid State Sci.* 4 (2002) 305.
- [6] L. Chi, A.E.C. Green, R. Hammond, C.R. Wiebe, J.E. Greedan, *J. Solid State Chem.* 170 (2003) 165.
- [7] L. Chi, I.P. Swainson, J.E. Greedan, *J. Solid State Chem.* 177 (2004) 3086.
- [8] T. Roisnel, J. Rodriguez-Carvajal, *Mater. Sci. Forum* 378–381 (2001) 118.
- [9] L.J. de Jongh, in: L.J. de Jongh (Ed.), *Magnetic Properties of Layered Transition Metal Compounds*, Kluwer Academic Publishers, Dordrecht, 1990, p. 19.
- [10] J.B. Goodenough, *Magnetism and the Chemical Bond*, Wiley, New York, 1963.
- [11] J. Kanamori, *Phys. Chem. Solids* 10 (1959) 87.